Estimation of Two-Dimensional Frequencies Using Modified Matrix Pencil Method

Fang-Jiong Chen, Carrson C. Fung, *Member, IEEE*, Chi-Wah Kok, *Senior Member, IEEE*, and Sam Kwong, *Senior Member, IEEE*

***Abstract*—The problem of multiple two-dimensional (2-D) sinusoidal frequency estimation is considered. A modified matrix pencil method is proposed to simultaneously estimate the frequency pairs in the signal, thereby bypassing the computationally expensive pairing operation as seen in the literature. Simulation results show that the accuracy of the estimates for each frequency from our technique is better than or comparable to that of existing methods and the variance of the estimates are close to the Cramér–Rao bound. Simulation results also show that our method provides accurate and consistent frequency estimation results that other methods cannot provide with less or comparable computational complexity.**

***Index Terms*—ESPRIT, frequency estimation, matrix pencil.**

I. Introduction

Two-dimensional (2-D) frequency estimation of multiple superimposed complex sinusoidal signals has applications in many areas such as wireless communications [1], radio astronomy, ultrasound imaging, sonar, and radar. The matrix enhancement and matrix pencil (MEMP) method [2] has been proposed to solve such an estimation problem. It estimates the 2-D sinusoidal signals separately in each dimension and then combines the frequency pairs using a pairing algorithm. Unfortunately, this method is computationally expensive. Furthermore, it does not always provide the correct pairing results when there are repeated frequencies. In this correspondence, we propose a modification of the MEMP method that alleviates the pairing problem. We call our algorithm the modified MEMP (MMEMP) method. Simulation results will show that the estimation accuracy of the individual frequencies from the MMEMP method is comparable to those in [2] and [3] with correct pairing, and it is better than the recently proposed 2-D ESPRIT method [4] in the case of low SNR, e.g., SNR $=$ 10 dB. We also show that the variance of the estimates from our proposed method is close to the Cramér–Rao bound. Simulation results also show that our pairing technique provides more accurate pairing results than the MEMP method and requires less computational complexity than the MEMP method.

Manuscript received July 11, 2005; revised March 19, 2006. The associate editor coordinating the review of this manuscript and approving it for publication was Dr. Soren Holdt Jensen. The work described in this paper has been supported by the NSF of China under grant 60402014, the Research Grants Council of Hong Kong, China (Project no. CERG HKUST6236/01E), and the City University Strategic Grant 7001615.

F.-J. Chen is with the School of Electronics and Information Engineering, South China University of Technology, Guangzhou, China, 51064 (e-mail: eefjchen@scut.edu.cn).

C. C. Fung is with the Department of Electronics Engineering, National Chiao Tung University, Hsinchu, Taiwan (e-mail: c.fung@ieee.org).

C.-W. Kok and S. Kwong are with the Department of Computer Science, City University of Hong Kong, Kowloon, Hong Kong (e-mail: eekok@ieee.org; cssamk@cityu.edu.hk).

Color versions of one or more of the figures in this paper are available online at http://ieeexplore.ieee.org.

Digital Object Identifier 10.1109/TSP.2006.885813

II. Methodology

The 2-D complex-valued sinusoidal signal under consideration is of the form

$$s(m,n)=\sum_{k=1}^{N_s}\alpha_k\exp\{j\phi_k+j2\pi f_{1k}m+j2\pi f_{2k}n\} \tag{1}$$

where $m=0,1,\ldots,M-1$, $n=0,1,\ldots,N-1$. N_s is the number of sinusoidal components we have. α_k, ϕ_k, and $\{f_{1k},f_{2k}\}$ are the amplitude, phase, and frequency pair for the kth signal, respectively. The observed signal $x(m,n)$ can be written as

$$x(m,n)=s(m,n)+\eta(m,n) \tag{2}$$

where $\eta(m,n)$ is a 2-D white Gaussian distributed noise. To simplify the notations, we shall rewrite (2) as $x(m,n)=\sum_{k=1}^{N_s}a_k y_k^m z_k^n+\eta(m,n)$, where $a_k=\alpha_k\exp\{j\phi_k\}$, $y_k=\exp\{j2\pi f_{1k}\}$, and $z_k=\exp\{j2\pi f_{2k}\}$. The estimation of the amplitude α_k and phase ϕ_k are regarded as separate problems and are not considered in this correspondence. Since part of the proposed method is similar to [2], we shall use the notations defined in [2] throughout the paper.

The MEMP method [2] considered an enhanced matrix $\mathbf{X}_e$ that contains a moving average of the signal $x(m,n)$. The frequency estimation problem is solved by investigating the eigenstructure of

$$\mathbf{X}_e=\sum_{k=1}^{J}\sigma_k\mathbf{u}_k\mathbf{v}_k^H=[\mathbf{U}_s\ \mathbf{U}_n]\begin{bmatrix}\Sigma_s & \mathbf{0}\\ \mathbf{0} & \Sigma_n\end{bmatrix}\begin{bmatrix}\mathbf{V}_s^H\\ \mathbf{V}_n^H\end{bmatrix}$$

with $J=\min(KL,(M-K+1)(N-L+1))$, and without loss of generality, we assume $\sigma_1\geq\sigma_2\geq\cdots\geq\sigma_J$. K and L are free adjustable parameters which are used to improve estimation performance. As a result, $\mathbf{U}_s$ and $\mathbf{U}_n$ span the signal and noise subspace, respectively. The MEMP method makes use of the singular vector $\mathbf{U}_s$ to construct a set of matrices that result in two pairs of matrix pencils such that the rank reducing number, or the generalized eigenvalues, are y_k and z_k for $k=1,2,\ldots,N_s$. Using this approach, the frequency f_{1k} can be estimated by computing the generalized eigenvalues of its corresponding pair of matrix pencil. In this correspondence, we shall show that the second frequency f_{2k} can be obtained by using the generalized eigenvector from the matrix pencil corresponding to f_{1k}. As a result, the proposed method will guarantee the estimated frequencies are paired up correctly.

We shall now develop the first pair of matrix pencils to estimate the first set of frequencies f_{1k}. As shown in [2], the matrix pencils are constructed by the matrices $\mathbf{U}_1$, $\mathbf{U}_2$, $\mathbf{E}_1$, and $\mathbf{Y}_d$. Readers who are interested in the development and definition of the above matrices should refer to [2]. The matrices $\mathbf{U}_1$ and $\mathbf{U}_2$ are related to the matrix $\mathbf{E}_1$ as

$$\mathbf{U}_1=\mathbf{E}_1\mathbf{T}\quad\text{and}\quad\mathbf{U}_2=\mathbf{E}_1\mathbf{Y}_d\mathbf{T} \tag{3}$$

where $\mathbf{T}$ is an unique $N_s\times N_s$ nonsingular matrix. From (3), we can write the matrix pencil $\mathbf{U}_2-\lambda\mathbf{U}_1$ as

$$\begin{aligned}&\mathbf{U}_2-\lambda\mathbf{U}_1=\mathbf{E}_1(\mathbf{Y}_d-\lambda\mathbf{I})\mathbf{T},\\ \text{or}\quad&(\mathbf{U}_2-\lambda\mathbf{U}_1)\mathbf{w}_k=[\mathbf{E}_1(\mathbf{Y}_d-\lambda\mathbf{I})\mathbf{T}]\mathbf{w}_k=0\end{aligned} \tag{4}$$

where $\mathbf{I}$ is the identity matrix of size $N_s \times N_s$, and λ and $\mathbf{w}_k$ are the generalized eigenvalue and eigenvector of the matrix pencils $\mathbf{U}_2 - \lambda\mathbf{U}_1$ and $\mathbf{E}_1(\mathbf{Y}_d - \lambda\mathbf{I})\mathbf{T}$, respectively. From [5], y_k is the generalized eigenvalue of the two matrix pencils in (4).

A. Distinct f_{1k}'s

Theorem 1: If $(\mathbf{U}_2 - \lambda\mathbf{U}_1)\mathbf{w}_k = [\mathbf{E}_1(\mathbf{Y}_d - \lambda\mathbf{I})\mathbf{T}]\mathbf{w}_k = 0$, then the generalized eigenvector matrix $\mathbf{W}$ for the matrix pencils $\mathbf{U}_2 - \lambda\mathbf{U}_1$ and $\mathbf{E}_1(\mathbf{Y}_d - \lambda\mathbf{I})\mathbf{T}$ is linearly related to the inverse of the matrix $\mathbf{T}$, that is

$$\mathbf{WG} = \mathbf{T}^{-1} \tag{5}$$

where $\mathbf{W} = [\mathbf{w}_1\ \mathbf{w}_2\ \ldots\ \mathbf{w}_{N_s}]$, and $\mathbf{G}$ is a full rank diagonal matrix which represents the scalar ambiguity between $\mathbf{W}$ and $\mathbf{T}$.

Proof: The matrix pencil, $(\mathbf{U}_2 - \lambda\mathbf{U}_1)\mathbf{w}_k$, can be written in matrix form as

$$\mathbf{U}_2\mathbf{W} = \mathbf{U}_1\mathbf{WY} \tag{6}$$

where $\mathbf{Y} = \mathrm{diag}(y_1', y_2', \ldots, y_{N_s}')$ is the generalized eigenvalue matrix of the matrix pencil $\mathbf{U}_2 - \lambda\mathbf{U}_1$. Note that the order of the diagonal elements in $\mathbf{Y}$ does not necessarily corresponds to those in $\mathbf{Y}_d$ even though both matrices contain the same diagonal elements, which explains the use of the notation y_k' for the elements of $\mathbf{Y}$. Without loss of generality, we can assume $\mathbf{Y} = \mathbf{Y}_d$ so that (6) can be rewritten as

$$\mathbf{U}_2\mathbf{W} = \mathbf{U}_1\mathbf{WY}_d. \tag{7}$$

Using (7), we can estimate the frequency f_{1k} from y_k by computing the eigenvalue matrix $\mathbf{Y}_d$.

If we multiply the pseudoinverse $\mathbf{U}_1^{\dagger} = \left(\mathbf{U}_1^H\mathbf{U}_1\right)^{-1}\mathbf{U}_1^H$ on the left side of (7), we can rewrite (7) as

$$\mathbf{U}_1^{\dagger}\mathbf{U}_2 = \mathbf{WY}_d\mathbf{W}^{-1} \Longrightarrow \mathbf{Y}_d = \mathbf{W}^{-1}\mathbf{U}_1^{\dagger}\mathbf{U}_2\mathbf{W}. \tag{8}$$

Using (8), we can solve for the frequency f_{1k} by computing the eigenvalue of $\mathbf{U}_1^{\dagger}\mathbf{U}_2$. If f_{1k} for all k are distinct, then the eigenvalue decomposition of $\mathbf{U}_1^{\dagger}\mathbf{U}_2$ will be unique. We shall discuss the case where some of the frequencies are repeated in the sequel.

From (4), we also have $\mathbf{E}_1\mathbf{Y}_d\,\mathbf{Tw}_k = \lambda\mathbf{E}_1\mathbf{Tw}_k$. To express the generalized eigenvalue and eigenvector in matrix form in terms of the matrix pencil, we have $\mathbf{E}_1\mathbf{Y}_d\,\mathbf{TW} = \mathbf{E}_1\mathbf{TWY}_d$. Similar to (8), we left-multiply both sides by the pseudoinverse of $\mathbf{E}_1$, denoted as $\mathbf{E}_1^{\dagger}$, to obtain

$$\mathbf{Y}_d\mathbf{TW} = \mathbf{TWY}_d \implies \mathbf{T}^{-1}\mathbf{Y}_d\mathbf{T} = \mathbf{WY}_d\mathbf{W}^{-1}. \tag{9}$$

From (8) and (9), we have

$$\mathbf{U}_1^{\dagger}\mathbf{U}_2 = \mathbf{T}^{-1}\mathbf{Y}_d\mathbf{T} = \mathbf{WY}_d\mathbf{W}^{-1}. \tag{10}$$

From (10), we can conclude that $\mathbf{W}$ and $\mathbf{T}^{-1}$ contain the eigenvectors of $\mathbf{U}_1^{\dagger}\mathbf{U}_2$ and their corresponding columns correspond to the same eigenvalues and therefore are proportional, which leads to (5). ■

We shall use the relationship in (5) to simultaneously estimate the second frequency f_{2k} with the estimated f_{1k}.

Similar to the matrix pencil derivation for $\mathbf{Y}_d$, we can derive similar matrix pencil relations to determine the second frequency, f_{2k}, as

$$\begin{aligned} &\mathbf{U}_{2P} - \lambda\mathbf{U}_{1P} = \mathbf{E}_{1P}(\mathbf{Z}_d - \lambda\mathbf{I})\mathbf{T}, \\ \text{or}\quad &(\mathbf{U}_{2P} - \lambda\mathbf{U}_{1P})\mathbf{r}_k = [\mathbf{E}_{1P}(\mathbf{Z}_d - \lambda\mathbf{I})\mathbf{T}]\mathbf{r}_k = 0 \end{aligned} \tag{11}$$

where $\mathbf{r}_k$ is the generalized eigenvector of the matrix pencils $\mathbf{U}_{2P} - \lambda\mathbf{U}_{1P}$ and $\mathbf{E}_{1P}(\mathbf{Z}_d - \lambda\mathbf{I})\mathbf{T}$. The matrix $\mathbf{Z}_d$ is the (diagonal) generalized eigenvalue matrix for the matrix pencils $\mathbf{U}_{2P} - \lambda\mathbf{U}_{1P}$ and $\mathbf{E}_{1P}(\mathbf{Z}_d - \lambda\mathbf{I})\mathbf{T}$ [2]. We can rewrite (11) as

$$\mathbf{U}_{1P}^{\dagger}\mathbf{U}_{2P} = \mathbf{RZ}_d\mathbf{R}^{-1} \tag{12}$$

where $\mathbf{U}_{1P}^{\dagger} = (\mathbf{U}_{1P}^H\mathbf{U}_{1P})^{-1}\mathbf{U}_{1P}^H$ and $\mathbf{R} = [\mathbf{r}_1\ \mathbf{r}_2\ \ldots\ \mathbf{r}_{N_s}]$. If f_{2k}'s are distinct, following the same argument as above, we can also conclude that the matrix $\mathbf{T}^{-1}$ contains the eigenvectors of $\mathbf{U}_{1P}^{\dagger}\mathbf{U}_{2P}$, and it is related to $\mathbf{R}$ by $\mathbf{R}\hat{\mathbf{G}} = \mathbf{T}^{-1}$ where $\hat{\mathbf{G}}$ is a full-rank diagonal matrix so that (12) becomes $\mathbf{U}_{1P}^{\dagger}\mathbf{U}_{2P} = \left(\hat{\mathbf{G}}\mathbf{T}\right)^{-1}\mathbf{Z}_d\hat{\mathbf{G}}\mathbf{T}$. Using (5), the above equation can be rewritten as

$$\mathbf{U}_{1P}^{\dagger}\mathbf{U}_{2P} = \mathbf{WZ}_d\mathbf{W}^{-1} \Longrightarrow \mathbf{Z}_d = \mathbf{W}^{-1}\mathbf{U}_{1P}^{\dagger}\mathbf{U}_{2P}\mathbf{W}. \tag{13}$$

If there are repeated f_{2k}'s, from (11), we still have $\mathbf{U}_{1P}^{\dagger}\mathbf{U}_{2P} = \mathbf{T}^{-1}\mathbf{Z}_d\mathbf{T}$, which implies $\mathbf{U}_{1P}^{\dagger}\mathbf{U}_{2P}$ has N_s linearly independent eigenvectors (the columns of $\mathbf{T}^{-1}$) and therefore its eigenvalue decomposition (EVD), as indicated by (12), exists. However, $\mathbf{R}$ may not be equal to $\mathbf{T}^{-1}$. Assuming there are Υ distinct eigenvalues, the corresponding columns in $\mathbf{R}$ and $\mathbf{T}^{-1}$ are proportional if the columns correspond to eigenvalues with multiplicity 1. In the case of repeated eigenvalues, the corresponding columns in $\mathbf{T}^{-1}$ are linear combination of those in $\mathbf{R}$ [7]. This relationship can be described by

$$\mathbf{RQ} = \mathbf{T}^{-1} \tag{14}$$

where $\mathbf{Q}$ is a block diagonal matrix of the form

$$\mathbf{Q} = \begin{bmatrix} \mathbf{Q}_1 & 0 & 0 & 0 \\ 0 & \mathbf{Q}_2 & 0 & 0 \\ 0 & 0 & \ddots & 0 \\ 0 & 0 & 0 & \mathbf{Q}_\Upsilon \end{bmatrix}. \tag{15}$$

The submatrix $\mathbf{Q}_\xi$, for $\xi = 1, 2, \ldots, \Upsilon$, corresponds to each distinct eigenvalue. For the eigenvalues with multiplicity 1, $\mathbf{Q}_\xi$ is a 1×1 identity matrix. For the eigenvalues with multiplicity $q > 1$, and $\mathbf{Q}_\xi$ is a $q \times q$ nonsingular matrix. From (5) and (14), we have $\mathbf{W} = \mathbf{RQG}^{-1}$. Applying it to (12), we have $\mathbf{W}^{-1}\mathbf{U}_{1P}^{\dagger}\mathbf{U}_{2P}\mathbf{W} = \mathbf{GQ}^{-1}\mathbf{Z}_d\mathbf{QG}^{-1}$. For the case where all f_{2k}'s are distinct, $\mathbf{Q}$ is a full rank diagonal matrix; thus, $\mathbf{W}^{-1}\mathbf{U}_{1P}^{\dagger}\mathbf{U}_{2P}\mathbf{W} = \mathbf{GZ}_d\mathbf{G}^{-1} = \mathbf{Z}_d$. For the repeated f_{2k} case, $\mathbf{Z}_d$ is a diagonal matrix with repeated diagonal elements, where the repeated diagonal elements with multiplicity q correspond directly with the $q \times q$ nonsingular submatrix $\mathbf{Q}_\xi$; thus, $\mathbf{Z}_d$ is commutative with respect to $\mathbf{Q}$, $\mathbf{Q}^{-1}$, $\mathbf{G}$, and $\mathbf{G}^{-1}$. As a result, $\mathbf{W}^{-1}\mathbf{U}_{1P}^{\dagger}\mathbf{U}_{2P}\mathbf{W} = \mathbf{Z}_d$.

This shows that no matter whether there are repeated f_{2k}'s or not, $\mathbf{Z}_d$ can be computed by premultiplying $\mathbf{U}_{1P}^{\dagger}\mathbf{U}_{2P}$ with $\mathbf{W}^{-1}$, and then postmultiplying with $\mathbf{W}$. From (8), since the same eigenvector matrix is also used to compute $\mathbf{Y}_d$, the diagonal elements of $\mathbf{Z}_d$ must correspond directly to those in $\mathbf{Y}_d$. From $\mathbf{Z}_d$, we can extract the frequency f_{2k}. As a result, we can estimate f_{1k} and f_{2k} simultaneously.

B. Repeated f_{1k}'s

Assume that there are Ψ distinct eigenvalues in $\mathbf{Y}_d$. Similar to (14), we have

$$\mathbf{W}\overline{\mathbf{Q}} = \mathbf{T}^{-1} \tag{16}$$

where $\overline{\mathbf{Q}}$ is also a block diagonal matrix of the form

$$\overline{\mathbf{Q}} = \begin{bmatrix} \overline{\mathbf{Q}}_1 & 0 & 0 & 0 \\ 0 & \overline{\mathbf{Q}}_2 & 0 & 0 \\ & & \ddots & 0 \\ 0 & 0 & 0 & \overline{\mathbf{Q}}_\Psi \end{bmatrix}. \tag{17}$$

The square matrix $\overline{\mathbf{Q}}_\psi$, for $\psi = 1, 2, \ldots, \Psi$, is a $q \times q$ nonsingular matrix that corresponds to each distinct eigenvalue of multiplicity q. From (14) and (16), we have $\mathbf{W} = \mathbf{R}\mathbf{Q}\overline{\mathbf{Q}}^{-1}$. Applying it to $\mathbf{U}_{1P}^{\dagger}\mathbf{U}_{2P}$, we have $\mathbf{W}^{-1}\mathbf{U}_{1P}^{\dagger}\mathbf{U}_{2P}\mathbf{W} = \overline{\mathbf{Q}}\mathbf{Q}^{-1}\mathbf{Z}_d\mathbf{Q}\overline{\mathbf{Q}}^{-1} = \overline{\mathbf{Q}}\mathbf{Z}_d\overline{\mathbf{Q}}^{-1}$. Decomposing $\mathbf{Z}_d$ according to the eigenvalues in $\mathbf{Y}_d$ as

$$\mathbf{Z}_d = \begin{bmatrix} \mathbf{Z}_1 & 0 & 0 & 0 \\ 0 & \mathbf{Z}_2 & 0 & 0 \\ & & \ddots & 0 \\ 0 & 0 & 0 & \mathbf{Z}_\Psi \end{bmatrix}$$

where $\overline{\mathbf{Q}}_\psi$ and $\mathbf{Z}_\psi$ have the same size; then we have

$$\overline{\mathbf{Q}}\mathbf{Z}_d\overline{\mathbf{Q}}^{-1} = \begin{bmatrix} \overline{\mathbf{Q}}_1\mathbf{Z}_1\overline{\mathbf{Q}}_1^{-1} & 0 & 0 & 0 \\ 0 & \overline{\mathbf{Q}}_2\mathbf{Z}_2\overline{\mathbf{Q}}_2^{-1} & 0 & 0 \\ & & \ddots & 0 \\ 0 & 0 & 0 & \overline{\mathbf{Q}}_\Psi\mathbf{Z}_\Psi\overline{\mathbf{Q}}_\Psi^{-1} \end{bmatrix}. \tag{18}$$

In the case where the eigenvalues in $\mathbf{Y}_d$ have multiplicity 1, $\overline{\mathbf{Q}}_\psi$ is an identity matrix of size 1×1; therefore, $\overline{\mathbf{Q}}_\psi\mathbf{Z}_\psi\overline{\mathbf{Q}}_\psi^{-1} = \mathbf{Z}_\psi$. The eigenvalues in $\mathbf{Y}_d$ and $\mathbf{Z}_d$ form a pair of estimated frequencies. In other cases where the eigenvalues in $\mathbf{Y}_d$ have multiplicity $q > 1$, $\overline{\mathbf{Q}}_\psi$ and $\mathbf{Z}_\psi$ are matrices of size $q \times q$. Defining $\mathbf{A}_\psi = \overline{\mathbf{Q}}_\psi\mathbf{Z}_\psi\overline{\mathbf{Q}}_\psi^{-1}$, we conclude that the corresponding z_ψ can be estimated as the eigenvalues of $\mathbf{A}_\psi$. Our conclusion is based on the fact that 1) the diagonal elements in $\mathbf{Z}_\psi$ are distinct and they are the eigenvalues of $\mathbf{A}_\psi$ and 2) the $q \times q$ matrix $\mathbf{A}_\psi$ cannot have more than q eigenvalues.

We use a simple example to illustrate how the algorithm is implemented. Assuming there are three distinct eigenvalues in $\mathbf{Y}_d$ and one of them is repeated, that is $\mathbf{Y}_d = \mathrm{diag}(y_1, y_2, y_3, y_3)$. As a result, (18) becomes

$$\overline{\mathbf{Q}}\,\overline{\mathbf{Z}}_d\overline{\mathbf{Q}}^{-1} = \begin{bmatrix} z_1 & 0 & 0 \\ 0 & z_2 & 0 \\ 0 & 0 & \mathbf{A}_3 \end{bmatrix}$$

where

$$\mathbf{A}_3 = \overline{\mathbf{Q}}_3 \begin{bmatrix} z_3 & 0 \\ 0 & z_4 \end{bmatrix} \overline{\mathbf{Q}}_3^{-1}.$$

.z_3 and z_4 can be obtained by computing the EVD of $\mathbf{A}_3$ where the eigenvalues are z_3 and z_4. Therefore, (y_1, z_1) and (y_2, z_2) form two frequency pairs and (y_3, z_3) and (y_3, z_4) form the other two.

C. Summary of Algorithm

1) Form the enhanced matrix, $\mathbf{X}_e$ using the observed data. Perform singular value decomposition (SVD) on $\mathbf{X}_e$ to obtain the matrices $\mathbf{U}_s$, $\mathbf{U}_1$, $\mathbf{U}_2$, $\mathbf{U}_{1P}$, and $\mathbf{U}_{2P}$.
2) Perform an EVD on the matrix $\mathbf{U}_1^{\dagger}\mathbf{U}_2$ to obtain the (diagonal) eigenvalue and eigenvector matrix $\mathbf{Y}_d$ and $\mathbf{W}$, respectively. $\mathrm{diag}(\mathbf{Y}_d)$ corresponds to the frequency f_{1k}.
3) Check if there is any repeated frequencies, f_{1k}. The following detection test can be used: if $(y_{k+1} - y_k)/y_k < \gamma$, then y_{k+1} and y_k are identical, where γ is a predefined threshold.

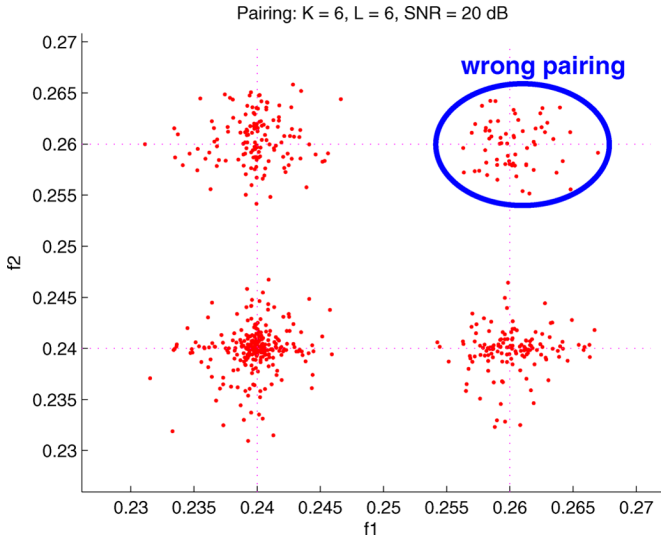

Fig. 1. MEMP: Two hundred independent estimates of three 2-D frequencies for $K = L = 6$, SNR = 20 dB when none of the incorrect pairs were thrown away.

4) Apply the eigenvector matrix, $\mathbf{W}$, to $\mathbf{U}_{1P}^{\dagger}\mathbf{U}_{2P}$ to obtain $\mathbf{Z}_d = \mathbf{W}^{-1}\mathbf{U}_{1P}^{\dagger}\mathbf{U}_{2P}\mathbf{W}$. $\mathrm{diag}(\mathbf{Z}_d)$ corresponds to the frequency f_{2k} if there are no repeated f_{1k}'s. If there are repeated f_{1k}'s, then for each repeated eigenvalue y_k, extract the corresponding block $\mathbf{A}_k$ in $\mathbf{Z}_d$. Perform an EVD on $\mathbf{A}_k$. Each eigenvalue of $\mathbf{A}_k$ and $\mathbf{y}_k$ corresponds to a pair of estimated frequencies.

III. Results

The observed signal in the following simulations is of the form

$$x(m,n) = \sum_{k=1}^{3} \exp\{j2\pi f_{1k}m + j2\pi f_{2k}n\} + \eta(m,n), \tag{19}$$

for $0 \le m \le 19$ and $0 \le n \le 19$. The noise signal $\eta(m,n)$ is white Gaussian distributed. We shall use the frequency pairs $(f_{11}, f_{21}) = (0.26, 0.24)$, $(f_{12}, f_{22}) = (0.24, 0.24)$, and $(f_{13}, f_{23}) = (0.24, 0.26)$ to illustrate the pairing problem that exists in the MEMP method and to show the estimation accuracy of our technique compared to that of the MEMP method and the 2-D ESPRIT method. Computational complexity between the MMEMP, the MEMP method and the 2-D ESPRIT method will also be compared. The signal-to-noise ratio (SNR) is defined as SNR $= 10\log(1/\sigma_\eta^2)$. Note that the definition of SNR here is different from [4] where the authors in [4] assumed that the signal power is equal to N_s rather than 1, as it is the case here.

In order to directly compare with the MEMP results in [2], [3], the modified enhanced matrix $\mathbf{X}_{ee} \triangleq [\mathbf{X}_{ee} \quad \mathbf{P}_e\mathbf{X}_e^*]$ ([2, eq. (5.7)]) is used in place of $\mathbf{X}_e$ for the MMEMP and 2-D ESPRIT methods to compute the frequencies f_{1k} and f_{2k}.

A. Pairing Problem With MEMP

The pairing operation in the MEMP method does not always render the correct pairing result because it is a correlation maximization algorithm. Fig. 1 shows the result for the MEMP method when $K = L = 6$ with SNR = 20 dB. As illustrated from the figure, the wrong pair (0.26, 0.26) was obtained using the MEMP method. The MMEMP method never experienced such a problem since the frequency pairs were estimated simultaneously using the same eigenvector matrix.

Next, we will compare the frequency estimation results using our MMEMP method developed in Section II with the MEMP method

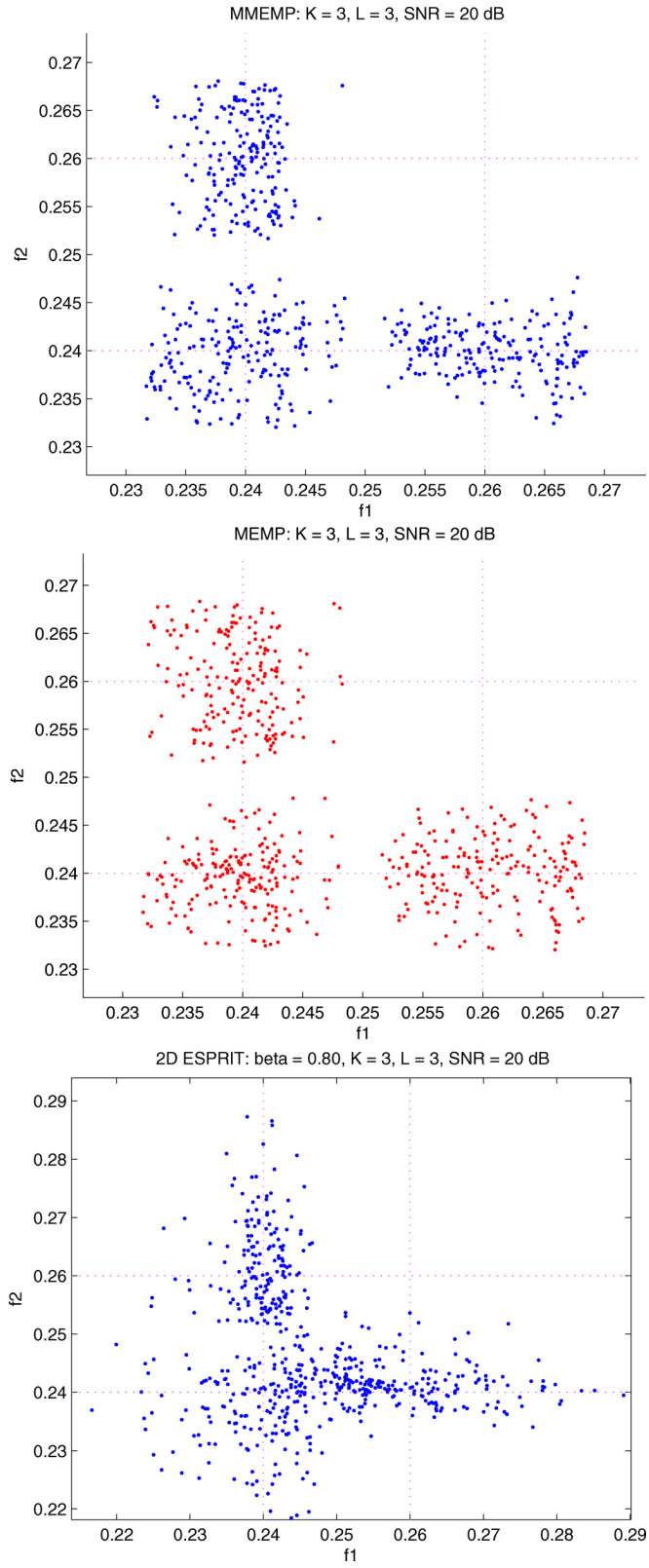

Fig. 2. Two hundred independent estimates of three 2-D frequencies for $K = L = 3$, SNR $= 20$ dB. From top to bottom: MMEMP, MEMP, and 2-D ESPRIT.

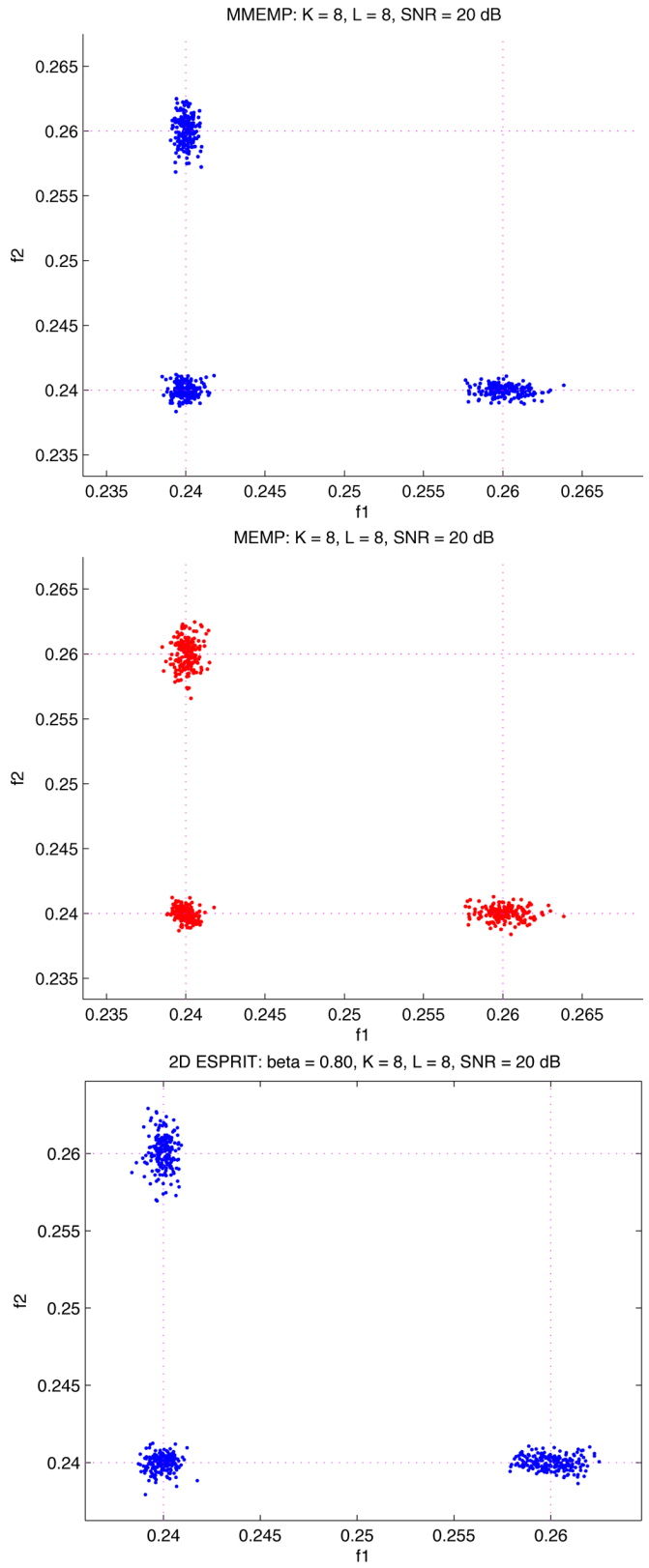

Fig. 3. Two hundred independent estimates of three 2-D frequencies for $K = L = 8$, SNR $= 20$ dB. From top to bottom: MMEMP, MEMP, and 2-D ESPRIT.

from [2] and the 2-D ESPRIT method in [4]. To obtain a fair comparison, only correct pairing results from the MEMP method were used. For the 2-D ESPRIT method, the parameter β is set to 0.8 as suggested in [4]. For other frequency pairs, however, another value for β might be needed to ensure that the combined matrices do not have repeated eigenvalues such that accurate frequency estimates can be obtained. As a result, the selection of a correct β value will either complicate the algorithm or reduce the estimation accuracy. The variance of

TABLE I
BIAS, DEVIATION AND CRB FOR THE MMEMP, MEMP, AND 2-D ESPRIT METHODS FOR 200 INDEPENDENT ESTIMATES FOR $K = L = 6, 8$, SNR = 20 dB

f_1	Bias ($\times 10^{-4}$)	Dev ($\times 10^{-3}$)	CRB ($\times 10^{-3}$)	f_2	Bias ($\times 10^{-4}$)	Dev ($\times 10^{-3}$)	CRB ($\times 10^{-3}$)
MMEMP method	(K=L=6, K=L=8)	(K=L=6, K=L=8)			(K=L=6, K=L=8)	(K=L=6, K=L=8)	
0.26	1.66, 0.91	1.23, 1.07	0.40	0.24	-0.03, -0.03	0.41, 0.40	0.32
0.24	-0.98, -0.31	0.79, 0.57	0.31	0.24	-0.17, -0.22	0.76, 0.53	0.31
0.24	0.29, 0.07	0.45, 0.41	0.32	0.26	0.93, 0.23	1.27, 1.08	0.40
MEMP method							
0.26	1.66, 0.91	1.23, 1.07	0.40	0.24	0.24, 0.17	0.69, 0.48	0.32
0.24	-0.17, -0.69	0.67, 0.47	0.31	0.24	-0.39, -0.31	0.62, 0.48	0.31
0.24	-0.53, 0.45	0.63, 0.51	0.32	0.26	0.89, 0.12	1.26, 1.08	0.40
2-D ESPRIT method							
0.26	1.05, 0.44	1.34, 1.01	0.40	0.24	0.12, 0.04	0.42, 0.43	0.32
0.24	-0.64, -0.61	0.80, 0.51	0.31	0.24	-0.03. -0.36	0.79, 0.51	0.31
0.24	-0.43, -0.07	0.43, 0.43	0.32	0.26	1.44, 0.62	1.35, 1.07	0.40

the estimates from the MMEMP method will also be compared to the Cramér–Rao bound (CRB) derived in [2].

B. Estimation Results

Figs. 2 and 3 show the estimation results for 200 independent estimates when the SNR = 20 dB with $K = L = 3$ and 8. From the figures, as K and L increase, the estimates become more accurate. Table I tabulates the bias and deviation (square root of the estimate's variance) of the estimates for the MMEMP, MEMP and 2-D ESPRIT methods and compare the deviation with the CRB when the SNR = 20 dB with $K = L = 6$ and $K = L = 8$. The results shown are averaged over 200 independent estimates. Note that the results for the MEMP method from Table I are comparable to those of [3], which are the corrected results of [2]. The results from the table reaffirm the results from the figures that as K and L increase, the estimates from all techniques become more accurate. As described in [2], this phenomenon can be intuitively explained by the inflating noise subspace concept because the noise subspace is expanded by increasing K and L so that more noise components are absorbed inside the noise subspace which result in increasing accuracy.

Figs. 4 and 5 show similar results for 200 independent estimates when the SNR = 10 dB with $K = L = 3$ and 8. As seen from the figures, the estimates are not as good as those in Figs. 2 and 3 when the SNR is 20 dB. When $K = L = 3$, none of the three methods can accurately estimate the frequencies. When K and L are increased to 8, both the MMEMP and MEMP are able to estimate the frequencies, albeit having a larger variance than that of the SNR = 20 dB case. However, the 2-D ESPRIT method fails to estimate all the frequency pairs accurately. This can be seen clearly from part (c) of Figs. 4 and 5 which is a zoom in picture of the estimates using the 2-D ESPRIT method.

As seen from Figs. 2–5, the estimation performance of the proposed MMEMP algorithm is comparable to that of the MEMP and it outperforms the 2-D ESPRIT method for low SNRs. This is shown more clearly by observing Table II where the performance for MMEMP, MEMP and 2-D ESPRIT are compared for the case of $K = L = 8$ with the SNR = 10 dB with $\beta = 0.8$ for the 2-D ESPRIT algorithm. From the table, not only is the estimation performance better for the MMEMP algorithm when compared to the 2-D ESPRIT algorithm, the estimates from the MMEMP also have less bias than that of the 2-D ESPRIT algorithm. Similar estimation performance between MMEMP and MEMP is expected because both algorithms extract the frequency information from the eigenvalue matrix of the matrix pencil. However, as we shall show below, the computational complexity of the MMEMP method is lower than that of the MEMP because the pairing procedure is eliminated. The 2-D ESPRIT method alleviates the pairing problem by linearly combining two matrices that have repeated frequencies in order to obtain a unique EVD for the repeated frequencies. As a result, the 2-D ESPRIT method does not require any pairing algorithm. However, the combined matrix in the 2-D ESPRIT method does not always have a unique EVD in the case of repeated frequencies and it requires the parameter β to be set to the correct value in order to obtain the correct decomposition. The criteria for choosing the right β was never discussed in [4]. This factor mainly attributed to less accurate estimates from the 2-D ESPRIT method as compared to the MMEMP and MEMP methods.

C. Complexity Analysis

Despite the similarities between the MMEMP and MEMP method, the MMEMP has an advantage in terms of computational complexity because it does not require an additional EVD to obtain $\mathbf{Z}_d$. Also it does not require a pairing operation because the components extracted from $\mathbf{Z}_d$ are already matched up with components from $\mathbf{Y}_d$. Therefore, we expect the MMEMP method to have less computational complexity than the MEMP method. The computational complexity of the 2-D ESPRIT method is similar to the MMEMP method since it requires the construction of the Hankel matrix and similar EVDs. However, as we shall illustrate below, the 2-D ESPRIT method requires an additional eigenvector multiplication in one of its steps.

For the three methods, an SVD is performed on the enhanced matrix $\mathbf{X}_e$ of dimension $KL \times (M-K+1)(N-L+1)$ to extract the signal space matrix $\mathbf{U}_s$. Assuming the fast method proposed in [2] is used, the number of multiplications is [6] $2KL(M-(K/2))(N-(L/2))+5K^3L$, for $K \gg 1$ and $L \gg 1$. As an engineering approximation, the much larger notation $\gg$ means at least ten times larger. This implies that K and L should be at least 10 for the complexity estimation to be valid. To simplify our simulation and keeping this assumption valid, we have chosen K and L to have a maximum value of 8. In fact, as stated in [2], the optimum value for K and L that maximize the noise subspace are $K = (M+1)/2$ and $L = (N+1)/2$. Since M and N are often very large, in order to keep the computational complexity to be tolerable, [2] suggested to choose K and L in the range of $N_s+1 \leq K \leq (M+1)/2$ and $N_s+1 \leq L \leq (N+1)/2$.

Instead of performing two EVDs as in the MEMP method, the MMEMP performs only one for the $\mathbf{U}_1^{\dagger}\mathbf{U}_2$ matrix plus two multiplications between the eigenvector matrices of $\mathbf{U}_1^{\dagger}\mathbf{U}_2$ and $\mathbf{U}_{1P}^{\dagger}\mathbf{U}_{2P}$. Obtaining the matrices $\mathbf{U}_1^{\dagger}\mathbf{U}_2$ and $\mathbf{U}_{1P}^{\dagger}\mathbf{U}_{2P}$ requires $3N_s^2KL$ number of multiplications. Assuming the QZ algorithm [6] is also used for the EVD, it requires $5N_s^3$ number of multiplication. Finally, the multiplications of the two eigenvectors require an additional $2N_s^3$ multiplications resulting in $3N_s^2KL+7N_s^3$ number of multiplications, assuming that there are no repeated frequencies and $K > N_s \gg 1$ and $L > N_s \gg 1$. If there are repeated frequencies, depending on how many different sets of repeated frequencies exist, each set will

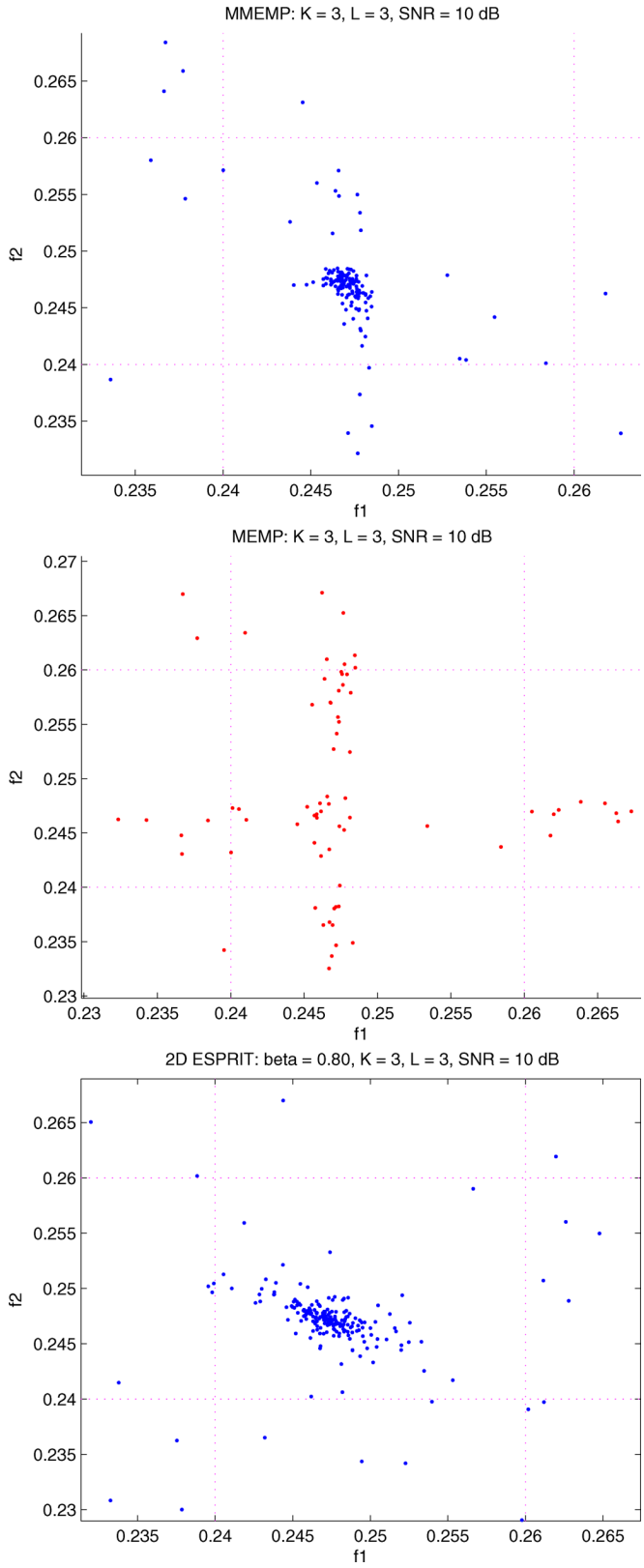

Fig. 4. Two hundred independent estimates of three 2-D frequencies for $K = L = 3$, SNR $= 10$ dB. From top to bottom: MMEMP, MEMP, and 2-D ESPRIT (zoomed in).

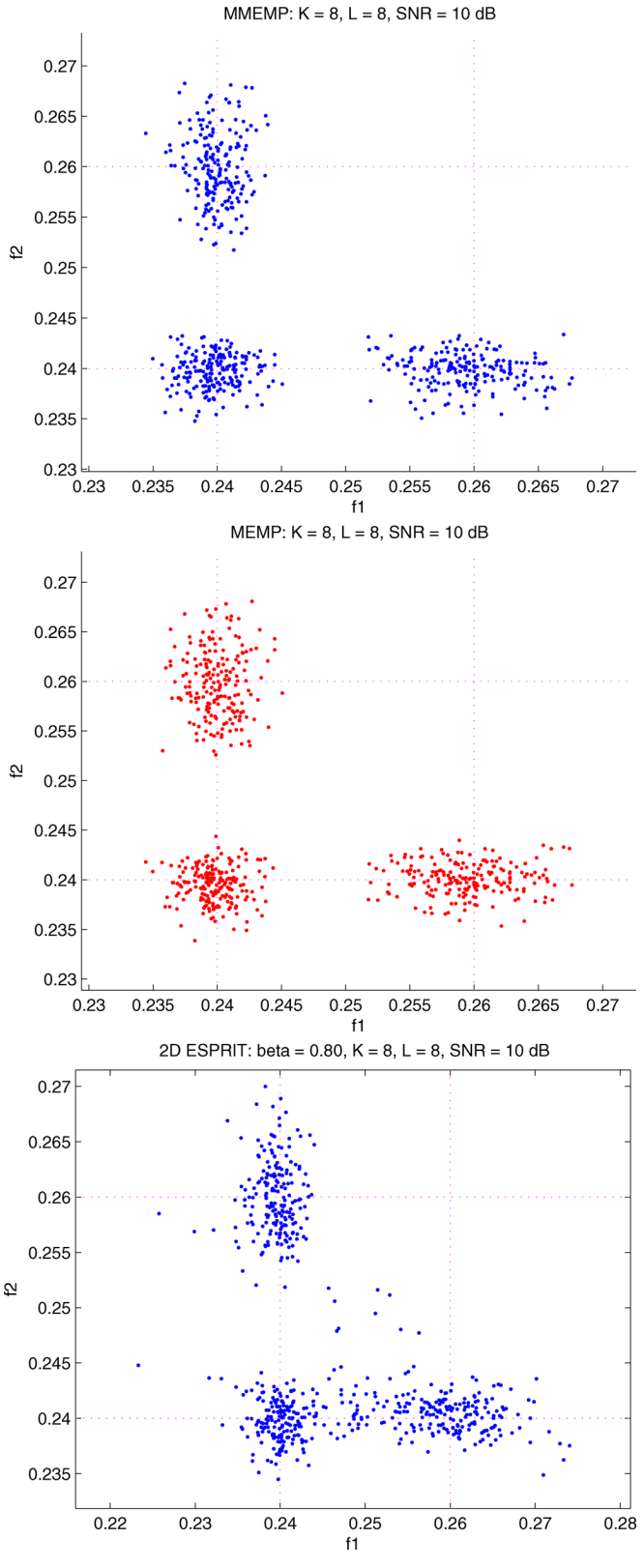

Fig. 5. Two hundred independent estimates of three 2-D frequencies for $K = L = 8$, SNR $= 10$ dB. From top to bottom: MMEMP, MEMP, and 2-D ESPRIT (zoomed in).

require an additional EVD, which will add an additional $5N_s^3$ number of multiplications. In the 2-D ESPRIT method, an extra eigenvector multiplication has to be carried out to decompose the two matrices, $\mathbf{F}_1$ and $\mathbf{F}_2'$, which results in an additional $2N_s^3$ multiplications compared to the MMEMP method, making the total number of multiplications to be $3N_s^2KL + 9N_s^3$.

TABLE II
BIAS, DEVIATION AND CRB FOR THE MMEMP, MEMP, AND 2-D ESPRIT METHODS FOR 200 INDEPENDENT ESTIMATES FOR $K = L = 8$, SNR = 10 dB

f_1	Bias ($\times 10^{-4}$)	Dev ($\times 10^{-3}$)	CRB ($\times 10^{-3}$)	f_2	Bias ($\times 10^{-4}$)	Dev ($\times 10^{-3}$)	CRB ($\times 10^{-3}$)
MMEMP method							
0.26	-6.03	3.41	1.30	0.24	-2.13	1.66	1.00
0.24	-1.87	1.94	1.00	0.24	-3.12	1.72	1.00
0.24	-0.39	1.56	1.00	0.26	-1.04	3.55	1.30
MEMP method							
0.26	-6.03	3.41	1.30	0.24	0.65	1.62	1.00
0.24	-2.53	1.77	1.00	0.24	-4.89	1.79	1.00
0.24	0.28	1.73	1.00	0.26	-2.07	3.42	1.30
2-D ESPRIT method							
0.26	-201	2.16	1.30	0.24	187	5.97	1.00
0.24	-105	11.4	1.00	0.24	10.4	3.80	1.00
0.24	98.90	12.0	1.00	0.26	-195	3.50	1.30

TABLE III
NUMBER OF MULTIPLICATIONS FOR THE MMEMP, MEMP AND 2-D ESPRIT METHODS ASSUMING NO REPEATED FREQUENCIES

	SVD of X_e	$\mathbf{U}_1^{\dagger}\mathbf{U}_2$ / $\mathbf{U}_{1P}^{\dagger}\mathbf{U}_{2P}$	Pairing
MMEMP	$2KL\left(M-\frac{K}{2}\right)\left(N-\frac{L}{2}\right)+5K^3L$	$3N_s^2KL+7N_s^3$	N/A
MEMP	$2KL\left(M-\frac{K}{2}\right)\left(N-\frac{L}{2}\right)+5K^3L$	$3N_s^2KL+10N_s^3$	$\frac{1}{2}N_s^3KL$
2-D ESPRIT	$2KL\left(M-\frac{K}{2}\right)\left(N-\frac{L}{2}\right)+5K^3L$	$3N_s^2KL+9N_s^3$	N/A

Table III summarizes the complexity of each of the operations for the MMEMP, MEMP and 2-D ESPRIT methods when $K > N_s \gg 1$, $L > N_s \gg 1$, $M, N \gg 1$. According to the table, the computational saving for our MMEMP method comes from performing one less EVD (3rd column in the table) when compared to the MEMP method, in the case when there are no repeated frequencies, and the elimination of the pairing operation. Since the parameters K and L are greater than the total number of components N_s, the computational complexity of our algorithm is comparable to that of the 2-D ESPRIT. Depending on how many sets of repeated frequencies there are, the complexity of the MMEMP might become comparable or even exceeds that of the MEMP and 2-D ESPRIT methods. However, for the MMEMP method, only additional EVDs are needed. Since the MMEMP algorithm does not require any search procedure, vector machine can be used in the implementation to speed up the computation. While the pairing operation in MEMP is a searching algorithm, using a vector machine will not provide any performance gain.

IV. CONCLUSION

We have proposed the modified matrix enhancement and matrix pencil method to deal with the 2-D frequency estimation problem. We have shown that our pairing technique always yields the correct frequency pairs as opposed to the MEMP and 2-D ESPRIT methods when there are repeated frequencies. For the 2-D ESPRIT method, an appropriate parameter β is required to be initiated before accurate results can be obtained. In the case of low SNR, e.g., SNR = 10 dB, our results show that the MMEMP and MEMP methods outperform the 2-D ESPRIT method in terms of estimation accuracy. Our results also show that if there are no repeated frequencies, then the MMEMP is computationally less complex than the MEMP method and of comparable complexity to the 2-D ESPRIT method.

REFERENCES

[1] A. J. van der Veen, M. C. Vanderveen, and A. Paulraj, "Joint angle and delay estimation using shift-invariance techniques," *IEEE Trans. Signal Process.*, vol. 46, no. 2, pp. 405–418, Feb. 1998.

[2] Y. Hua, "Estimating two-dimensional frequencies by matrix enhancement and matrix pencil," *IEEE Trans. Signal Process.*, vol. 40, no. 9, pp. 2267–2280, Sep. 1992.

[3] Y. Hua and F. Baqai, "Correction to estimating two-dimensional frequencies by matrix enhancement and matrix pencil," *IEEE Trans. Signal Process.*, vol. 42, no. 5, p. 1288, May 1994.

[4] S. Rouquette and M. Najim, "Estimation of frequencies and damping factors by two-dimensional ESPRIT type methods," *IEEE Trans. Signal Process.*, vol. 49, no. 1, pp. 237–245, Jan. 2001.

[5] Y. Hua and T. K. Sarkar, "Matrix pencil method for estimating parameters of exponentially damped/undamped sinusoids in noise," *IEEE Trans. Acoustics, Speech, Signal Process.*, vol. 38, no. 5, pp. 814–824, May 1990.

[6] G. H. Golub and C. F. Van Loan, *Matrix Computations*, 3rd ed. Baltimore, MD: The Johns Hopkins Univ. Press, 1996.

[7] G. Strang, *Linear Algebra and Its Applications*, 3rd ed. San Diego, CA: Harcourt Brace Jovanovich, 1988.